

تقنية جديدة لتقدير مقاومة الشبكة لمحولات الطاقة المتصلة بالشبكة

ز.جاو، ز.لو، ز.سن، هـ. جو، و.وو
قسم الهندسة الكهربائية، جامعة يانشان، الصين

الخلاصة

إن معرفة مقاومة الشبكة مهم جداً لعمليات التشغيل والتحكم في المحولات المتصلة بالشبكة خاصة مع الاختراق الكبير لمصادر الطاقة المتجددة في الشبكات المصغرة والذكية. إحدى التحديات التقنية هي مدى سرعة ودقة قياس مقاومة الشبكة وخاصة في ظروف التشويش وعدم الإتران. توجد عدة طرق لقياس مقاومة الشبكة ومعظمها يعتمد على حقن إشارات مؤثرة ذات تردد عالي أو منخفض لإثارة ردة فعل الشبكة. ومن ثم يمكن قياس مقاومة الشبكة عن طريق معلومات فرق الجهد والتيار لحالتي مستقرتين قبل وبعد الإثارة. ولكن هذه الطريقة سوف تؤدي إلى تدهور جودة الطاقة نتيجة الموجات التي تسببها عملية الحقن. حتى يمكن حل هذه المشكلة تم استخدام الطريقة الجديدة المبينة في هذه الورقة. تكمن الفكرة الأساسية لهذه الطريقة في خاصية التبادل لمحولات الطاقة المرتبطة بالشبكة. الخاصية الفريدة لهذه الطريقة أنه يمكن قياس مقاومة الشبكة تحت أي ظروف دون الحاجة لحقن إشارة. أولاً يتم تحليل المقاومة المكافئة للدائرة لتوضيح الطريقة المقترحة وبالمقارنة النظرية مع الدائرة التقليدية. وبجانب ذلك تم عرض طريقة قياس مثيرة لفرق الجهد وعناصر تبادل التيار المستخدمة لتقدير مقاومة الشبكة بواسطة معادلتين معرفتين تماماً. تم عمل فحص الأداء ودعمت النتائج فعالية الطريقة المقترحة. وأخيراً تم عرض تطبيق تقليدي للطريقة المقترحة وتم نقاشها.

New grid impedance estimation technique for grid-connected power converters

XIAOQIANG GUO, ZHIGANG LU, XIAOFENG SUN, HERONG GU
AND WEIYANG WU

*Department of Electrical Engineering, Yanshan University, China,
Corresponding Author: Xiaoqiang Guo, gxq@ysu.edu.cn*

ABSTRACT

Grid impedance estimation is crucial for operating and controlling of grid-connected converters, especially with the high penetration of renewable energy sources into microgrid and smart grid. One of the technical challenges is how to fast and accurately estimate the grid impedance, even under the distorted and unbalanced conditions. Many impedance estimation methods have been presented in the past decades. Most of them intentionally inject one or more disturbance signals, low frequency or high frequency, to excite the grid response. And then the grid impedance can be estimated by the voltage/current information of two steady-state operating points before and after the disturbance. However, these injected disturbances will deteriorate the power quality due to harmonics caused by the injected disturbances. In order to mitigate the problem, a new impedance estimation method is presented in this paper. Its basic idea lies in the inherent switching feature of the grid-connected power converter. The unique feature is that the proposed new grid impedance can be easily estimated, even under distorted and unbalanced grid voltage conditions with no need of the intentionally injected disturbance signals any more. First of all, the system equivalent impedance circuit is analyzed to clarify the proposed method, along with a theoretical comparison with the conventional one. Aside from that, an interesting estimation of voltage and current switching components are presented for determining the grid impedance with two well-defined equations. And then, the performance tests are carried out and the results verify the effectiveness of the proposed method. Finally, a typical application of the proposed method is presented and discussed.

Keywords: Distributed power generation; grid-connected converter; grid impedance; impedance estimation; islanding; microgrid.

INTRODUCTION

Nowadays, the integration of renewable energy resources and distributed power generation into grid is getting more and more attention (Guerrero *et al.*, 2013, 2011; Zhong & Hornik, 2013; Li & Chen, 2008). With the high penetration of renewable power generation systems in the microgrid and smart grid, many technical challenges should be dealt with before successful grid integration. One of the most important issues is how to fast and accurately estimate the grid impedance. In practice, the impedance information is of particular concern because it leads to interactions between the grid-connected

power converters and the grid, which might cause the system resonance and instability (Sun, 2011). Aside from that, the impedance information is also essential for many other applications, such as power sources and conditioners design (Roberto, 2009), islanding detection (Ciobotaru *et al.*, 2010), power flow control (Vasquez *et al.*, 2009), passive filter design (Das, 2004), and active filter control (Tarkiainen *et al.*, 2004).

Generally, impedance estimation methods can be mainly classified into two categories: invasive and noninvasive methods. The latter one usually measures the excitation of the natural load variations to calculate the impedance (Bien *et al.*, 2007). It is theoretically simple and does not need to intentionally inject disturbance signals. So there is no power quality degradation problem. However, the successful and accurate impedance estimation is highly dependent on the sufficient excitation response, which is not always the case in practice. On the other hand, the invasive method intentionally injects one or more disturbance signals, low frequency (Asiminoaei *et al.*, 2005; Timbus *et al.*, 2007) or high frequency (Summner *et al.*, 2004; Staroszczyk, 2005), periodically or randomly, to excite the grid response. And then the grid impedance can be estimated by the voltage/current information of two steady-state operating points before and after the disturbance. However, these injected disturbances will deteriorate the power quality due to harmonics and inter-harmonics caused by the injected disturbances (Asiminoaei *et al.*, 2005). Also in medium or high voltage grid, the disturbance injection device should be powerful enough to excite the grid response, which is not cost effective in practice. In order to solve this problem, the passive load, resistive or capacitive, is stepped to generate the grid excitation (Valdivia *et al.*, 2011). Besides, some unique solutions have been presented for grid impedance estimation. An interesting approach presented by Liserre *et al.* (2007) is to estimate the grid impedance by the excitation of the LCL-filter resonance. The impedance information can also be identified according to the cross coupling of d-axis and q-axis currents, as reported in Kulka & Undeland (2008).

In this paper, a new grid impedance estimation method is presented, which is an extension of our conference paper (Gu *et al.*, 2012). It utilizes the inherent switching feature of the grid-connected power converter to excite the grid response. So the grid impedance can be easily estimated with no need of the intentionally injected disturbance signals any more. The theoretical analysis and performance evaluation are presented to verify the proposal. Finally, a typical application of the proposed method is presented and discussed.

PROPOSED METHOD

Figure 1 illustrates the schematic diagram of grid-connected power converter system, where U_c and U_g are the converter-side and grid-side voltages respectively. Z_g is the equivalent impedance of the grid. L_1 is the converter-side inductor.

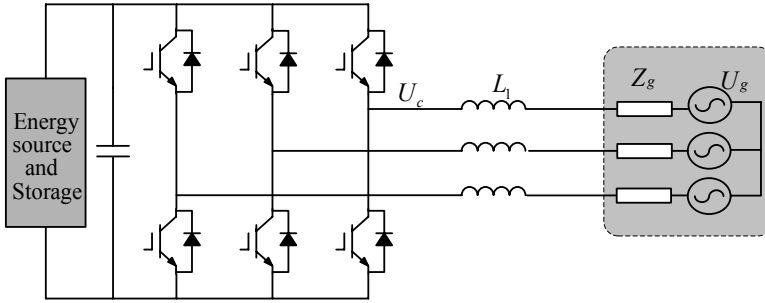


Fig. 1. Schematic diagram of grid-connected power converter system.

Considering the switching feature of the power converter, the converter-side voltage U_c can be represented by the pulse waveform, and thus Figure 1 can be simplified as shown in Figure 2.

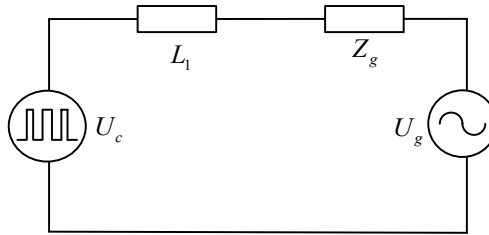


Fig. 2. Simplified diagram of Fig.1

It is known that any periodic signal can be represented as the sum of harmonically-related sinusoidal waves. Therefore, the converter-side and grid-side voltages can be expressed as (1), and then Figure 2 is further simplified as shown in Figure 3.

$$U_c = \sum U_{ch} \text{ and } U_g = \sum U_{gh} . \tag{1}$$

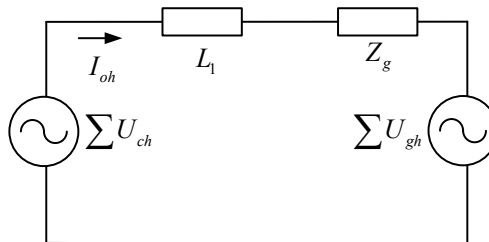


Fig. 3. Equivalent diagram of Fig.2

Conventional method

The grid impedance at a specific frequency can be calculated from Figure 3 as follows:

$$Z_g = \frac{U_{ch} - U_{gh}}{I_{oh}} - L_1 \quad (2)$$

where I_{oh} , U_{ch} and U_{gh} are the grid current, converter and grid voltage components at a specific frequency respectively.

From (2), it can be concluded that the information of the converter voltage, grid current and the grid voltage should be available to calculate the grid impedance. However, in practice, the grid voltage is difficult to measure directly due to the long line distance. That is why the “two-sampling-point” (TSP) algorithm is widely used for the grid impedance calculation (Vasquez *et al.*, 2009; Timbus *et al.*, 2007; Staroszczyk, 2005). The basic idea of TSP algorithm is briefly explained as follows:

$$Z_g = \frac{U_{ch1} - U_{gh1}}{I_{oh1}} - L_1 = \frac{U_{ch2} - U_{gh2}}{I_{oh2}} - L_1 \quad (3)$$

where I_{oh1} , U_{ch1} and U_{gh1} are the grid current vectors, converter and grid voltage vectors at one steady-state sampling point respectively. I_{oh2} , U_{ch2} and U_{gh2} are the grid current vectors, converter and grid voltage vectors at another steady-state sampling point respectively.

With the mathematical manipulation, equation (3) can be rewritten as:

$$Z_g = \frac{(U_{ch1} - U_{ch2}) - (U_{gh1} - U_{gh2})}{I_{oh1} - I_{oh2}} - L_1 \quad (4)$$

Assuming that grid voltage remains unchanged between the sampling intervals, that is $U_{gh1} = U_{gh2}$, the grid impedance can be derived from (4) as follows:

$$Z_g = \frac{(U_{ch1} - U_{ch2})}{I_{oh1} - I_{oh2}} - L_1 = \frac{\Delta U_{ch}}{\Delta I_{oh}} - L_1 \quad (5)$$

Compared with (2), equation (5) indicates that the grid impedance calculation is not dependent on the grid voltage at all, but only on the local information such as the grid current and converter voltage, which can be easily obtained in practice.

Proposed method

The abovementioned “two-sampling-point” algorithm usually intentionally injects one or more disturbance signals to excite the grid response. However, these injected

disturbances will deteriorate the power quality due to harmonics and inter-harmonics caused by injected disturbances (Asiminoaei *et al.*, 2005). Also, the impedance estimation delay is highly dependent on the response time from the initial injection to another steady-state point (Vasquez *et al.*, 2009). In order to mitigate the problem, a new impedance estimation method is presented in this paper. It utilizes the inherent switching feature of the grid-connected power converter to excite the grid response. So the grid impedance can be easily estimated with no need of the intentionally injected disturbance signals any more. The basic idea of the proposed algorithm is briefly explained as follows.

It is known that the high frequency voltage harmonics are rare in the practical power systems, because the voltage harmonic magnitude tends to decrease as the frequency increases. So, it is reasonable to assume that there is no high frequency (e.g. above 10 kHz) harmonics in the grid voltage. In this case, equation (2) can be rewritten as:

$$Z_{gs} = \frac{U_{cs} - U_{gs}}{I_{os}} - j\omega L_1 = \frac{U_{cs}}{I_{os}} - j\omega L_1 \quad (6)$$

where I_{os} , U_{cs} and U_{gs} are the grid current, converter and grid voltages at the frequency associated with the switching feature of power converters.

From (6), it can be concluded that the grid impedance can be calculated by the local information. More specifically, equation (6) can be expressed with the instantaneous complex vectors (e.g. $U = U_{\alpha} - jU_{\beta}$, $I = I_{\alpha} - jI_{\beta}$, $Z = R + j\omega L$).

$$Z_{gs} = \frac{U_{cs\alpha} - jU_{cs\beta}}{I_{os\alpha} - jI_{os\beta}} - j\omega L_1 = \frac{(U_{cs\alpha}I_{os\alpha} + U_{cs\beta}I_{os\beta}) + j(U_{cs\alpha}I_{os\beta} - U_{cs\beta}I_{os\alpha})}{I_{os\alpha}^2 + I_{os\beta}^2} - j\omega L_1 \quad (7)$$

It is clear that the grid impedance can be easily obtained from (7) as follows:

$$R = \frac{U_{cs\alpha}I_{os\alpha} + U_{cs\beta}I_{os\beta}}{I_{os\alpha}^2 + I_{os\beta}^2} \quad (8)$$

$$L = \frac{U_{cs\alpha}I_{os\beta} - U_{cs\beta}I_{os\alpha}}{\omega(I_{os\alpha}^2 + I_{os\beta}^2)} - L_1 \quad (9)$$

Note that the R can be easily calculated with the instantaneous variables of converter voltage and grid current. On the other hand, L_1 is already known for a well-designed converter filter, and L is dependent on the angular frequency ω . Therefore, the excited frequency should be determined in advance.

Considering the inherent switching feature of the grid-connected power converter, the excited frequency is mainly determined by the pulse-width modulation. The

frequency-spectra characteristic analysis of the pulse-width modulation (PWM) process has been reported in Holmes & McGrath (2001), where the phase voltage can be expressed in the following form:

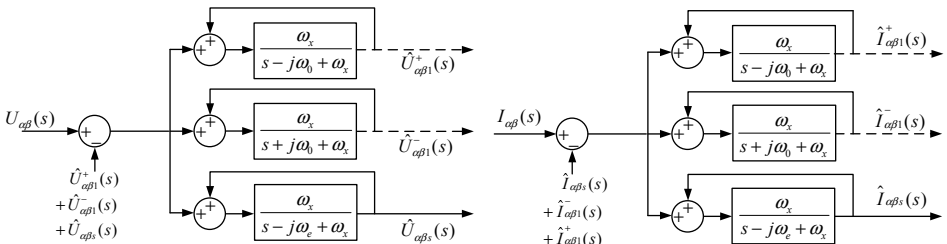
$$U_c = V_{dc}M \cos(\omega_0 t - k \frac{2\pi}{3}) + \frac{4V_{dc}}{\pi} \sum_{m=1}^{\infty} \sum_{n=-\infty}^{\infty} \frac{1}{m} \{ \sin([\frac{\pi}{2} + m + n] \frac{\pi}{2}) J_n(m \frac{\pi}{2} M) \cos(m[\omega_c t] + n[\omega_0 t - k \frac{2\pi}{3}]) \} \quad (10)$$

where M is the modulation index, V_{dc} is the dc-link voltage, J_n is the Bessel function, ω_0 is the angular frequency of modulation signal, which is the same as the grid voltage angular frequency, ω_c is the angular frequency of PWM carrier signal. In the following, ω_e is the excited angular frequency, which is defined as $\omega_c - 2\omega_0$. ω_x is the cutoff angular frequency of the multiple complex coefficient filters (MCCF).

As mentioned before, the excited frequency in the paper is mainly determined by the pulse-width modulation. The excited frequency can be determined by (10), which indicates that the mainly harmonic components are located at $\omega_c \pm 2\omega_0$. For simplicity of analysis, the excited angular frequency ω_e is chosen as $\omega_c - 2\omega_0$.

Instantaneous variables measurement

In order to successfully estimate the grid impedance even under distorted and unbalanced conditions, the voltage and current components at the excited frequency should be available in advance. For example, equation (8) and (9) indicate that the grid current and converter voltage should be known for the grid impedance estimation. It can be achieved by the MCCF structure (Guo *et al.*, 2011), as shown in Figure 4, where $U_{\alpha\beta}(s)$ and $I_{\alpha\beta}(s)$ are the voltage and current components at the measurement point. $\hat{I}_{\alpha\beta 1}^+(s)$ and $\hat{I}_{\alpha\beta 1}^-(s)$ are the estimated fundamental current components. $\hat{U}_{\alpha\beta 1}^+(s)$ and $\hat{U}_{\alpha\beta 1}^-(s)$ are the estimated fundamental voltage components, which are used for grid synchronization under distorted and unbalanced conditions. $\hat{U}_{\alpha\beta s}(s)$ and $\hat{I}_{\alpha\beta s}(s)$ are the estimated voltage and current components at the excited frequency, which are used for the grid impedance calculation.



(a) Voltage component extraction

(b) Current component extraction

Fig. 4. Voltage and current component extraction

The mathematical model of the voltage component extraction structure can be obtained from Figure 4 as follows.

$$\left\{ \begin{array}{l} \hat{U}_{\alpha 1}^+(s) = \frac{\omega_x}{s - j\omega_0 + \omega_x} [U_\alpha(s) - U_{\alpha 1}^-(s) - U_{\alpha s}(s)] \\ \hat{U}_{\beta 1}^+(s) = \frac{\omega_x}{s - j\omega_0 + \omega_x} [U_\beta(s) - U_{\beta 1}^-(s) - U_{\beta s}(s)] \\ \hat{U}_{\alpha 1}^-(s) = \frac{\omega_x}{s + j\omega_0 + \omega_x} [U_\alpha(s) - U_{\alpha 1}^+(s) - U_{\alpha s}(s)] \\ \hat{U}_{\beta 1}^-(s) = \frac{\omega_x}{s + j\omega_0 + \omega_x} [U_\beta(s) - U_{\beta 1}^+(s) - U_{\beta s}(s)] \\ \hat{U}_{\alpha s}(s) = \frac{\omega_x}{s - j\omega_e + \omega_x} [U_\alpha(s) - U_{\alpha 1}^+(s) - \hat{U}_{\alpha 1}^-(s)] \\ \hat{U}_{\beta s}(s) = \frac{\omega_x}{s - j\omega_e + \omega_x} [U_\beta(s) - U_{\beta 1}^+(s) - \hat{U}_{\beta 1}^-(s)] \end{array} \right. \quad (11)$$

The corresponding time-domain equation of (11) can be derived as (12).

$$\left\{ \begin{array}{l} \dot{\hat{U}}_{\alpha 1}^+(s) = \omega_x [U_\alpha(s) - U_{\alpha 1}^+(s) - U_{\alpha 1}^-(s) - U_{\alpha s}(s)] - \omega_0 U_{\beta 1}^+(s) \\ \dot{\hat{U}}_{\beta 1}^+(s) = \omega_x [U_\beta(s) - U_{\beta 1}^+(s) - U_{\beta 1}^-(s) - U_{\beta s}(s)] + \omega_0 U_{\alpha 1}^+(s) \\ \dot{\hat{U}}_{\alpha 1}^-(s) = \omega_x [U_\alpha(s) - U_{\alpha 1}^-(s) - U_{\alpha 1}^+(s) - U_{\alpha s}(s)] + \omega_0 U_{\beta 1}^-(s) \\ \dot{\hat{U}}_{\beta 1}^-(s) = \omega_x [U_\beta(s) - U_{\beta 1}^-(s) - U_{\beta 1}^+(s) - \hat{U}_{\beta s}(s)] - \omega_0 U_{\alpha 1}^-(s) \\ \dot{\hat{U}}_{\alpha s}(s) = \omega_x [U_\alpha(s) - U_{\alpha 1}^+(s) - U_{\alpha 1}^-(s) - U_{\alpha s}(s)] - \omega_e U_{\beta s}(s) \\ \dot{\hat{U}}_{\beta s}(s) = \omega_x [U_\beta(s) - U_{\beta 1}^+(s) - U_{\beta 1}^-(s) - U_{\beta s}(s)] + \omega_e U_{\alpha s}(s) \end{array} \right. \quad (12)$$

The state-space model can be derived from (12) as (13).

$$\left\{ \begin{array}{l} \dot{x}(t) = A(t) \cdot x(t) + B(t) \cdot u(t) \\ y(t) = C \cdot x(t) \end{array} \right. \quad (13)$$

$$\text{where } x(t) = y(t) = [\hat{U}_{\alpha 1}^+ \ U_{\beta 1}^+ \ U_{\alpha 1}^- \ U_{\beta 1}^- \ U_{\alpha s} \ U_{\beta s}] \quad u(t) = [U_\alpha \ U_\beta \ U_\alpha \ U_\beta \ U_\alpha \ U_\beta]^T$$

$$A(t) = \begin{bmatrix} -\omega_x & -\omega_0 & -\omega_x & 0 & -\omega_x & 0 \\ \omega_0 & -\omega_x & 0 & -\omega_x & 0 & -\omega_x \\ -\omega_x & 0 & -\omega_x & -\omega_0 & -\omega_x & 0 \\ 0 & -\omega_x & \omega_0 & -\omega_x & 0 & -\omega_x \\ -\omega_x & 0 & -\omega_x & 0 & -\omega_x & -\omega_e \\ 0 & -\omega_x & 0 & -\omega_x & \omega_e & -\omega_x \end{bmatrix}_{6 \times 6} \quad B(t) = \begin{bmatrix} \omega_x & 0 & 0 & 0 & 0 & 0 \\ 0 & \omega_x & 0 & 0 & 0 & 0 \\ 0 & 0 & \omega_x & 0 & 0 & 0 \\ 0 & 0 & 0 & \omega_x & 0 & 0 \\ 0 & 0 & 0 & 0 & \omega_x & 0 \\ 0 & 0 & 0 & 0 & 0 & \omega_x \end{bmatrix}_{6 \times 6} \quad C = I_{6 \times 6}$$

The time-domain solution of (13) can be written as (14).

$$x(t) = e^{A(t-t_0)}x(t_0) + \int_{t_0}^t e^{A(t-\tau)}Bu(\tau)d\tau \quad (14)$$

The full mathematical expression for the time-domain solution of (14) is too complex to describe here. But it can be concluded that its transient response mainly depends on the cutoff frequency of ω_x . The dynamic response time of the proposed technique presented in Figure 4 can be controlled within half a cycle (10ms), as reported in Guo, *et al.* (2011). It will be beneficial to the fast grid impedance estimation.

On the other hand, the steady-state solution to (14) is (15).

$$x(t) = \begin{bmatrix} \hat{U}_{\alpha 1}^+ \\ \hat{U}_{\beta 1}^+ \\ \hat{U}_{\alpha 1}^- \\ \hat{U}_{\beta 1}^- \\ \hat{U}_{\alpha s} \\ \hat{U}_{\alpha s} \end{bmatrix} = \begin{bmatrix} U_{\alpha 1}^+ \\ U_{\beta 1}^+ \\ U_{\alpha 1}^- \\ U_{\beta 1}^- \\ U_{\alpha s} \\ U_{\alpha s} \end{bmatrix} \quad (15)$$

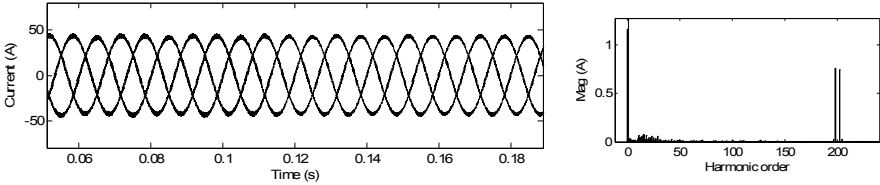
From the above theoretical analysis, it can be observed that the structure can be used to extract the voltage components, as well as current components, which are used for the grid impedance calculation.

System control structure

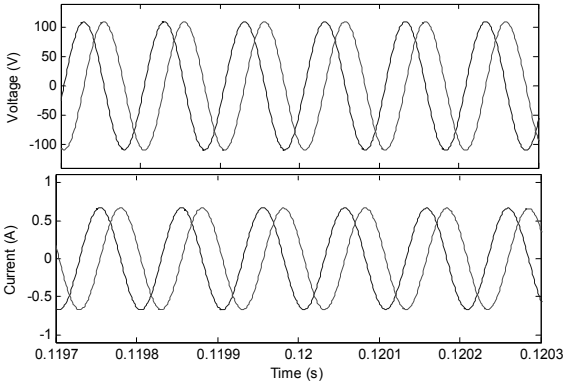
Figure 5 shows the single-line diagram of the system control structure. It can be divided into two main functions. One is for the system control, and the other is for the grid impedance estimation.

First of all, the grid current I_{abc} and converter voltage U_{abc} are measured. With the Clarke transformation, $U_{\alpha\beta}$ and $I_{\alpha\beta}$ are obtained. And then, the converter voltage and grid current components at the excited frequency ($U_{\alpha\beta s}$ and $I_{\alpha\beta s}$) can be extracted by the structure in Figure 4. Finally, the grid impedance can be easily estimated with (8) and (9).

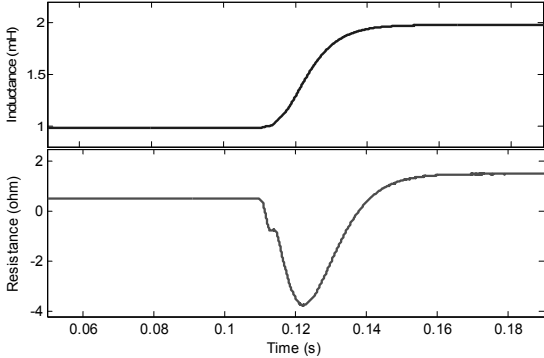
On the other hand, the system control structure is crucial for operating grid-connected power converter. The direct output current control (Guo, *et al.*, 2010) is used for the grid-connected power converter to enhance the system steady-state and dynamic performances. Aside from that, an additional impedance $R_{g2} + jL_{g2}$ and two switches (S1 and S2) are used for testing the dynamic performance of the proposed impedance estimation method. More specifically, when S1 is on and S2 is off, the grid impedance Z_g is $R_{g1} + jL_{g1}$. While S2 is on and S1 is off, the grid impedance Z_g



(c) Grid current



(d) Estimated instantaneous components at switching frequency



(e) Estimated grid impedance

Fig.6. Performance evaluation result under ideal grid voltage conditions

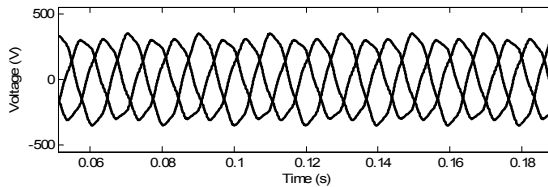
From Figure 6b, it can be observed that the high frequency harmonics of the converter voltage mainly locate at the angular frequency of $\omega_c \pm 2\omega_0$, which is in agreement with the theoretical analysis above. On the other hand, the harmonics at $\omega_c \pm 2\omega_0$ appear in the grid current due to the inherent switching feature of the converter, as shown in Figure 6c. Figure 6d illustrates the instantaneous variables information of the converter voltage and grid current at the excited frequency. It is clear that the proposed structure can provide the accurate information for grid

impedance estimation. The grid impedance estimation results are shown in Figure 6e, from which it can be observed that the grid impedance can be accurately estimated.

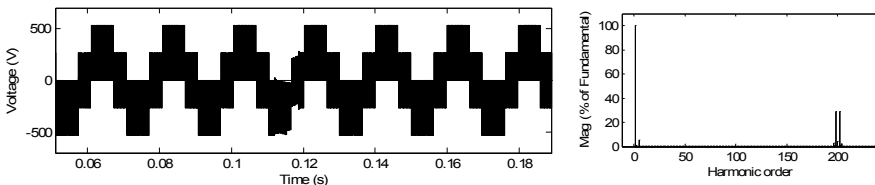
Figure 6 has presented the evaluation results under the ideal grid voltage condition. However, in practice, the grid might be polluted with harmonics due to many different types of loads connected to the grid. More severely, the grid even might experience the balance or unbalance grid faults. In addition, the random noises are common during the grid impedance measurement process. Therefore, it is of particular concern, whether the proposed method works well or not under the distorted/unbalanced grid and noise conditions. In the following, the tests will be carried out under distorted/unbalanced grid conditions, along with the zero mean white Gaussian noises are superposed on the current and voltage components to emulate the measurement noise. The variance of the noise is $\sigma^2 = 0.05$, which corresponds to a signal-to-noise ratio (SNR) 10 dB.

Nonideal conditions

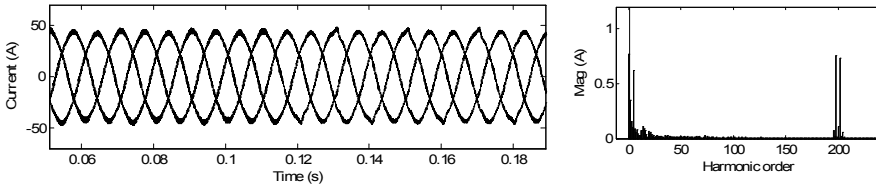
The evaluation results under the distorted/unbalanced grid voltage and noise conditions are shown in Figure 7. It is clear that the grid impedance estimation is satisfactory with the proposed method. Other further considerations should be noted, such as non-ideal switching behavior, sensors accuracy, etc, can make the negative influence on the performance of the proposed technique. For non-ideal switching behaviors, e.g. dead time, turn on/off delay and voltage drop across switching devices, the negative effect can be mitigated by the advanced strategy (Zhao *et al.*, 2004; Choi *et al.*, 2007). On the other hand, for improving the accuracy of the proposed impedance estimation method in practical applications, there are two possible solutions. One is to use the high precise sensors. It is reasonable and feasible in practice with the fast development of the advanced sensors (Rietveld *et al.*, 2009; Callegaro *et al.*, 2006). The other is to use the windows and interpolation algorithms to improve electrical measurement accuracy (Andria *et al.*, 1989).



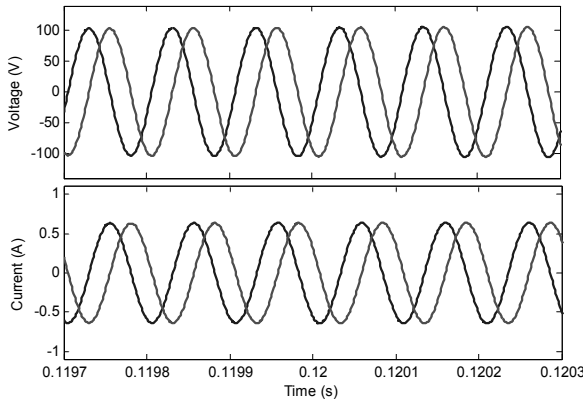
(a) Grid voltage



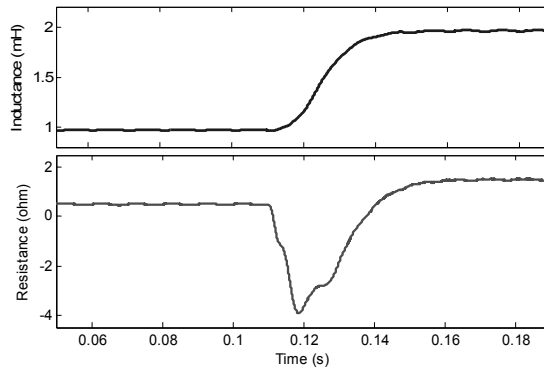
(b) Converter voltage



(c) Grid current



(d) Estimated instantaneous components at switching frequency



(e) Estimated grid impedance

Fig.7. Performance evaluation results under nonideal conditions

TYPICAL APPLICATION

As mentioned earlier, the grid impedance estimation is essential for many applications. Following will present a typical application to verify the effectiveness of the proposed method. Figure 8 shows the diagram of the islanding detection with the proposed grid impedance estimation method.

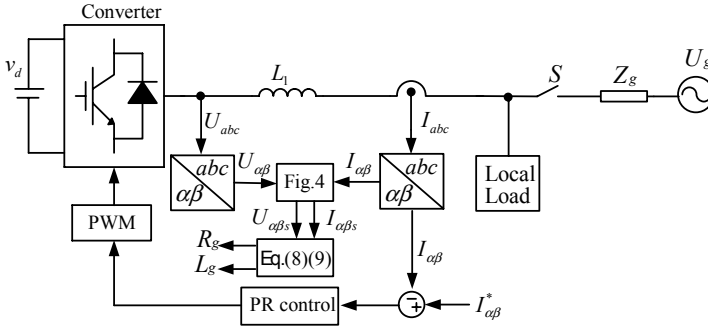
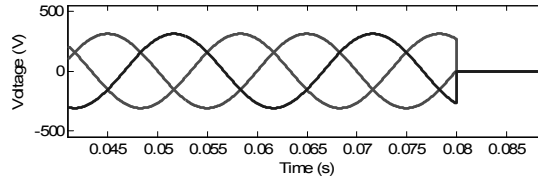
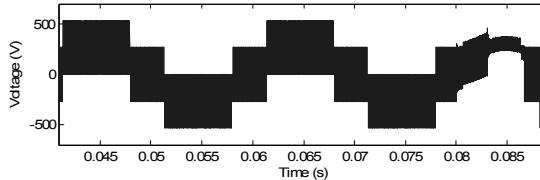


Fig. 8. Single-line diagram of the islanding detection

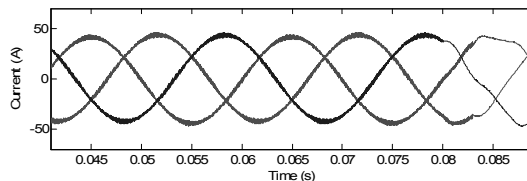
As we know, islanding occurs when the grid-connected converter and local load are disconnected from the grid, but the converter continues to energize the local load, which may result in many problems (Liu *et al.*, 2010). Therefore, it is essential to detect the islanding in a fast way. The European standard EN50330-1 specifies the ENS requirement of confirming islanding after an impedance change, which is reasonable because the local load impedance is much larger than the grid impedance. Figure 9 shows the evaluation results. At 0.08s, the grid is disconnected, only the converter energizes the local load, and the estimation impedance is greatly increased, which confirms the islanding. In contrast to the exiting islanding detection method, the proposed method can achieve the fast islanding detection with no need of the intentionally injected disturbance signals any more.



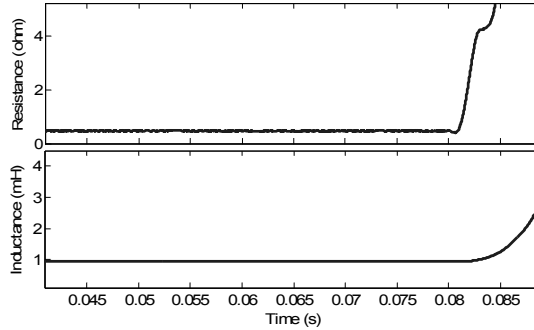
(a) Grid voltage



(b) Converter voltage



(c) Grid current



(d) Estimated grid impedance

Fig.9. Performance evaluation results of a typical application

CONCLUSION

This paper has presented a new grid impedance estimation method. It utilizes the inherent switching feature of the grid-connected power converter to excite the grid response. Therefore, the grid impedance can be easily estimated with no need of the intentionally injected disturbance signals any more. The proposed new method can achieve the fast and accurate estimation of the grid impedance, even under the distorted and unbalanced grid conditions. Therefore, it is very attractive in grid-connected power converter applications, e.g. active filter control, impedance stability analysis, islanding detection, and so on.

ACKNOWLEDGMENT

This work was supported by National Natural Science Foundation of China (51307149), China Postdoctoral Science Foundation (2014M551050), Hebei Province Education Department Excellent Young Scholars Foundation (YQ2014010) and Specialized Research Fund for Doctoral Program of Higher Education (20131333120016).

REFERENCES

- Andria, G., Savino, M. & Trotta, A. 1989.** Windows and interpolation algorithms to improve electrical measurement accuracy. *IEEE Transactions on Instrumentation and Measurement*, **38**(4): 856–863.
- Asiminoaei, L., Teodorescu, R., Blaabjerg, F. & Borup, U. 2005.** Implementation and test of an online embedded grid impedance estimation technique for PV inverters. *IEEE Transactions on Industrial Electronics*. **52**(4): 1136–1144.
- Bien, A., Borkowski, D., & Wetula, A. 2007.** Estimation of power system parameters based on load variance observations - laboratory studies. in *Proceedings of EPQU*.
- Choi, C., Cho, K & Seok, J. 2007.** Inverter nonlinearity compensation in the presence of current measurement errors and switching device parameter uncertainties. *IEEE Transactions on Power Electronics*. **22**(2): pp. 576–583.

- Callegaro, L., Delia, V., Capra, P. & Sosso, A. 2007.** Techniques for traceable measurements of small currents. *IEEE Transactions on Instrumentation and Measurement*, **56**(2): 295–299.
- Ciobotaru, M., Agelidis, G., Teodorescu, R. & Blaabjerg, F. 2010.** Accurate and less-disturbing active antiislanding method based on PLL for grid-connected converters. *IEEE Transactions on Power Electronics*. **25**(6): 1576-1584.
- Das, J. 2004.** Passive filters-potentialities and limitations. *IEEE Transactions on Industry Applications*. **40**(1): 232-241.
- Gu, H., Guo, X., Wang, D., & Wu, W. 2012.** Real-time grid impedance estimation technique for grid-connected power converters. *IEEE International Symposium on Industrial Electronics*, pp. 1621-1626.
- Guerrero, J. M., Chandorkar, M., Lee, T. L. & Loh, P. C. 2013.** Advanced control architectures for intelligent microgrids-Part I: Decentralized and hierarchical control. *IEEE Transactions on Industrial Electronics*. **60**(4): 1254-1262.
- Guerrero, J. M., Loh, P. C., Lee, T. L. & Chandorkar, M. 2013.** Advanced control architectures for intelligentmicrogrids-Part II: Power quality, energy storage, and AC/DC microgrids. *IEEE Transactions on Industrial Electronics*. **60**(4): 1263-1270.
- Guerrero, J. M., Vasquez, J. C., Matas, J., Vicuna, L. G. & Castilla, M. 2011.** Hierarchical control of droop-controlled AC and DC microgrids-A general approach toward standardization. *IEEE Transactions on Industrial Electronics*. **58**(1): 158-172.
- Guo, X., Wu, W. & Chen, Z. 2011.** Multiple-complex coefficient-filter based phase-locked loop and synchronization technique for three-phase grid-interfaced converters in distributed utility networks. *IEEE Transactions on Industrial Electronics*. 1194-1204.
- Guo, X., Wu, W. & Gu, H. 2010.** Modeling and simulation of direct output current control for LCL-interfaced grid-connected inverters. *Simulation Modelling Practice and Theory*, **18**: 946–956.
- Holmes, D. & McGrath, B. 2001.** Opportunities for harmonic cancellation with carrier-based PWM for a two-level and multilevel cascaded inverters. *IEEE Transactions on Industry Applications*. **37** (2): 574–582.
- Kulka, A. & Undeland, T. 2008.** Grid inductance estimation by reactive power perturbation for sensorless scheme based on virtual flux. in *Proceeding NORPIE*, 1-7.
- Li, H. & Chen, Z. 2008.** Overview of different wind generator systems and their comparisons. *IET Renewable Power Generation*, **2**(2): 123-138.
- Liserre, M., Blaabjerg, F. & Teodorescu, R. 2007.** Grid impedance estimation via excitation of LCL-filter resonance. *IEEE Transactions on Industry Applications*. **43**(5): 1401-7.
- Liu, F., Kang, Y., Zhang, Y., Duan, S. & Lin, X. 2010.** Improved SMS islanding detection method for grid-connected converters, *IET Renewable Power Generation*. **4**(2): 36-42.
- Rietveld, G., Court, P. & Brom, H. 2009.** Internally damped CCC for accurate measurements of small electrical currents. *IEEE Transactions on Instrumentation and Measurement*, **58**(4): 1196–1201.
- Roberto, E. 2009.** Output impedance measurement in low-power sources and conditioners. *IEEE Transactions on Instrumentation and Measurement*. **58**(1): 180-6.
- Staroszczyk, Z. 2005.** A method for real-time, wide-band identification of the source impedance in power systems. *IEEE Transactions on Instrumentation and Measurement*, **54**(1): 377-385.
- Sumner, M., Palethorpe, B., & Thomas, D. 2004.** Impedance measurement for improved power quality-part I: the measurement technique. *IEEE Transactions on Power Delivery*, **19**(3): 1442-8.
- Sun, J. 2011.** Impedance-based stability criterion for grid-connected inverters. *IEEE Transactions on Power Electronics*. **26** (11):3075-8.
- Tarkiainen, A., Pollanen, R., Niemela, M., & Pyrhonen, J. 2004.** Identification of grid impedance for purposes of voltage feedback active filtering. *IEEE Power Electronics Letters*, **2**(1): 6-10.

- Timbus, A. V., Rodriguez, P., Teodorescu, R. & Ciobotaru, M. 2007.** Line impedance estimation using active and reactive power variations. in Proc. of PESC, 1273-9.
- Valdivia, V., Lazaro, A., Barrado, A., Zumel, P., Fernandez, C. & Sanz, M. 2011.** Impedance identification procedure of three-phase balanced voltage source inverters based on transient response measurements. IEEE Transactions on Power Electronics. **26**(12): 3810-6.
- Vasquez, J. C., Guerrero, J. M., Luna, A., Rodriguez, P. & Teodorescu, R. 2009.** Adaptive droop control applied to voltage-source inverters operating in grid-connected and islanded modes. IEEE Transactions on Industrial Electronics. **56**(10): 4088-4096.
- Zhao, H., Wu, J. & Kawamura, A. 2004.** An accurate approach of nonlinearity compensation for VSI inverter output voltage. IEEE Transactions on Power Electronics. **19**(4): 1029-1035.
- Zhong, Q.-C. & Hornik, T. 2013.** Control of Power Inverters in Renewable Energy and Smart Grid Integration. New York, NY, USA: Wiley.

Open Access: This article is distributed under the terms of the Creative Commons Attribution License (CC-BY 4.0) which permits any use, distribution, and reproduction in any medium, provided the original author(s) and the source are credited.

Submitted: 27/03/2014

Revised: 06/05/2014

Accepted: 21/05/2014

مجلة العلوم الاجتماعية

فصلية - أكاديمية - محكمة

صدر عن مجلس النشر العلمي - جامعة الكويت

تعنى بنشر الأبحاث والدراسات في تخصصات السياسة والاقتصاد والاجتماع والخدمة الاجتماعية وعلم النفس والأنثروبولوجيا الاجتماعية والجغرافيا وعلوم المكتبات والمعلومات



رئيس التحرير: هادي مختار أشكناني

تفتح أبوابها أمام

توجه جميع المراسلات إلى:

رئيس تحرير مجلة العلوم الاجتماعية

جامعة الكويت

ص.ب. 27780 الصفاة، 13055 - الكويت

تليفون: 00965-4810436

فاكس 4836026

E-mail: JSS@kuc01.kuniv.edu.kw

أوسع مشاركة للباحثين العرب في مجال

العلوم الاجتماعية لنشر البحوث الأصيلة
والإسهام في معالجة قضايا مجتمعاتهم

التفاعل الحي مع القارئ المثقف والمهتم
بالقضايا المطروحة.

المقابلات والمناقشات الجادة
ومراجعات الكتب والتقارير.

تؤكد المجلة إلتزامها بالوفاء والانتظام بوصولها في
مواعيدها المحددة إلى جميع قرائها ومشتريها.

الإشتراكات

الدول الأجنبية

15 دولاراً

أفراد

60 دولاراً في السنة
110 دولارات لسنتين

مؤسسات

الكويت والدول العربية

3 دنانير سنوياً ويضاف إليها
دينار واحد في الدول العربية

أفراد

15 ديناراً في السنة
25 ديناراً لمدة سنتين

مؤسسات

تدفع اشتراكات الأفراد مقدماً نقداً أو بشيك باسم المجلة مسجوباً على أحد المصارف الكويتية ويرسل على عنوان المجلة، أو بتحويل مصرفي لحساب مجلة العلوم الاجتماعية رقم 07101685 لدى بنك الخليج في الكويت (فرع العديلية).

Visit our web site: <http://pubcouncil.kuniv.edu.kw/jss>